

SLIP AND DRAG IN TURBULENT FLOWS OVER SUPERHYDROPHOBIC SURFACES WITH SURFACTANT

Samuel D. Tomlinson

Department of Mathematics
University of Manchester
Oxford Rd, Manchester M13 9PL, UK
samuel.tomlinson@manchester.ac.uk

Ruby Gans

Department of Mechanical Engineering
University of California, Santa Barbara
Santa Barbara CA 93106, USA
rubygans@ucsb.edu

Frederic Gibou

Department of Mechanical Engineering
University of California, Santa Barbara
Santa Barbara CA 93106, USA
fgibou@ucsb.edu

Oliver E. Jensen

Department of Mathematics
University of Manchester
Oxford Rd, Manchester M13 9PL, UK
oliver.jensen@manchester.ac.uk

Julien R. Landel

Department of Mathematics
University of Manchester
Oxford Rd, Manchester M13 9PL, UK
julien.landel@manchester.ac.uk

Paolo Luzzatto-Fegiz

Department of Mechanical Engineering
University of California, Santa Barbara
Santa Barbara CA 93106, USA
fegiz@engineering.ucsb.edu

François Peaudecerf

Institute of Environmental Engineering
ETH Zürich
8063 Zürich, Switzerland
peaudecerf@ifu.baug.ethz.ch

Fernando Temprano-Coleto

Department of Mechanical Engineering
University of California, Santa Barbara
Santa Barbara CA 93106, USA
fempranocoleto@ucsb.edu

ABSTRACT

Superhydrophobic surfaces (SHSs) can reduce friction drag in turbulent flows. In the laminar regime, it has been shown that trace amounts of surfactant can negate this drag reduction, at times rendering these surfaces no better than solid walls (Peaudecerf *et al.* (2017)). However, surfactant effects on the drag-reducing properties of SHSs have not yet been studied under turbulent flow conditions. Predicting the effects of surfactant in numerical simulations remains expensive by today's standards. We present a model for turbulent flow, in either a channel or boundary layer, over a periodic array of longitudinal ridges (of period P and gas fraction ϕ) inclusive of surfactant. To acquire an expression for the drag reduction, we adopt a technique based upon a shifted log law. The homogenised streamwise and spanwise slip lengths are derived by introducing a local laminar model within the viscous sub-layer, whereby the effect of surfactant is modelled by modifying the streamwise slip length. We compare the predictions of our model with numerical and experimental results from the literature and discuss the potential effect of surfactants on turbulent flows over SHSs. Our model agrees with available data for small P^+ (subscript $+$ denotes wall units), showing a clear departure at large P^+ , where the drag reduction data asymptotically approach ϕ for $P^+ \rightarrow \infty$.

INTRODUCTION

SHSs owe their performance to a combination of hydrophobic chemistry and surface roughness, which acts to entrap gas layers in their surface and reduce the drag when compared to solid walls. Harnessing this feature in turbulent flows could benefit numerous marine and industrial applications. Maritime shipping alone contributes to over 2% of CO₂ emissions, and over 13% of NO_x and SO_x emissions (Smith *et al.* (2015)), with up to 80% of the energy expended to overcome friction drag (Fukuda *et al.* (2000); Xu *et al.* (2020)). Early investigations into the laminar regime modelled the SHS as a mixture of no-slip and shear-free boundaries (where the liquid-gas interface is assumed flat), thereby predicting large reductions in drag (Rothstein (2010)). However, more recent experimental studies in laminar flow conditions have shown that trace amounts of surfactant, unavoidable in practice, can strongly impair the drag-reducing effect of SHSs (Kim & Hidrovo (2012); Bolognesi *et al.* (2014); Peaudecerf *et al.* (2017); Song *et al.* (2018)). Motivated by these experimental findings, laminar theories have been developed for the fluid and surfactant in channels bounded by SHSs (Landel *et al.* (2020); Temprano-Coleto *et al.* (2021)), where it has been shown that model predictions can be improved relative to surfactant-free theories.

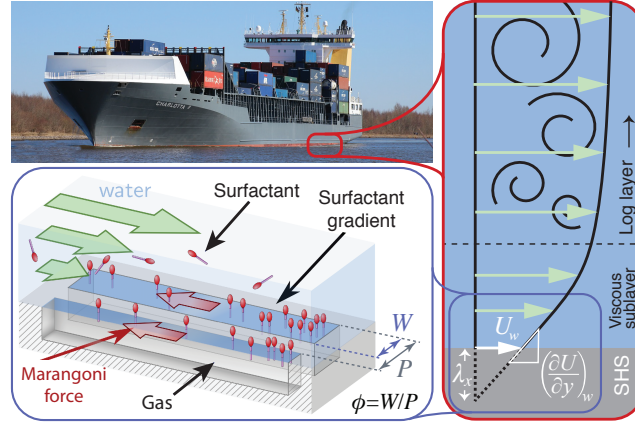


Figure 1. The mechanism by which the presence of surfactant can negatively impact the drag reduction for a flow over a SHS, with period P , gas ridge (plastron) width W and gas fraction $\phi = W/P$. A build up of surfactant at the downstream stagnation point induces an adverse Marangoni force due to the reduction in surface tension (Peaudecerf *et al.* (2017)). The adverse Marangoni force acts to reduce the spanwise-averaged streamwise slip length λ_x and slip velocity U_w at the interface. The smaller spanwise-averaged streamwise slip length (or slip velocity) reduces the drag reduction when compared to a surfactant-free flow over a SHS.

Numerous studies have investigated the performance of SHSs, both experimentally (Daniello *et al.* (2009); Park *et al.* (2014); Xu *et al.* (2021)) and computationally (Park *et al.* (2013); Türk *et al.* (2014); Rastegari & Akhavan (2015)), in turbulent flows without added surfactant. A recent review of 14 experiments shows broad inconsistencies (Gose *et al.* (2018)); the drag reduction ranges from -90% (i.e. drag increase) to $+90\%$, with five studies finding little ($< 20\%$) or no drag reduction. There exist a number of possible causes for this disagreement in the literature due to the complicated physics associated with flows over SHSs, which are discussed in detail in Park *et al.* (2021). As an example, the liquid-gas interface at the SHS can deform due to pressure differences in the bulk fluid and gas cavity, which has been shown to alter the drag reduction in laminar flows depending on the sign and magnitude of the protrusion angle (Teo & Khoo (2009)). Alternatively, turbulence may induce partial or complete wetting of the plastron containing the gas subphase, where the flow would no longer benefit from a shear-free surface (Rastegari & Akhavan (2019)). We neglect both these features of SHSs here, as apart from in certain asymptotic limits (see, for example, Crowdy (2017)), the laminar solutions found in the viscous sublayer would need to be found numerically.

This study aims to investigate the potential effects of surfactant in turbulent flow conditions, for both internal and external geometries, over longitudinally ridged SHSs (see Figure 1). We consider longitudinal ridges only as they are generally considered optimal when compared to transverse ridges, pillars or random surface roughness (Park *et al.* (2021)). We assume the liquid-gas interfaces are flat and can be approximated as shear-free, which allows us to relate the geometry of the SHS to the drag reduction using a technique based on a shifted log law (Fukagata *et al.* (2006)).

SHS PERFORMANCE

There are two main quantities of interest that characterize the local and global performance of the SHS flow compared to a no-slip flow over solid walls. Firstly, the spanwise-averaged

longitudinal slip length is commonly defined as

$$\lambda_x = \frac{U_w}{\gamma_w}, \quad (1)$$

where U_w is the spanwise-averaged slip velocity at the SHS boundary $y = 0$ and γ_w is the spanwise-averaged shear rate at $y = 0$ (see Figure 1 and 2). The average longitudinal slip length λ_x represents the extrapolated distance, below the SHS, where the time-averaged longitudinal velocity U vanishes (see Figure 1).

Secondly, for flows under the constant flow rate condition (equivalent to $U = U_0$, where U and U_0 are the cross-plane average velocities for the flow over a SHS and a solid wall respectively), we define the drag reduction

$$DR = \frac{\tau_0 - \tau}{\tau_0}, \quad (2)$$

where τ is the spanwise-averaged wall shear stress of the SHS flow, and τ_0 is the spanwise-averaged wall shear stress of the no-slip flow. Alternatively, the SHS and no-slip flows can be driven by imposing the same constant pressure gradient, such that the average shear stresses at the boundaries in both flows are equal (Türk *et al.* (2014)). To evaluate the global performance of a SHS geometry, the relationship between the drag reduction and the relevant independent non-dimensional parameters is sought in the form $DR = f(Re, P/H, \phi)$, where Re is the Reynolds number, P is the pitch, H is the channel height (which is replaced by the boundary layer thickness δ_b , if we are considering external flows such as Park *et al.* (2014); Xu *et al.* (2021)) and $\phi = G/P$ is the gas fraction, with G the plastron width (see Figure 2).

MODEL

As noted earlier, turbulent flows can be characterised by two regions of variation: an inner viscous sublayer and an outer log-law layer (see Figure 1). We assume that the viscous sublayer thickness, of order $10\delta_\tau$ (where $\delta_\tau = \nu/u_\tau$ is

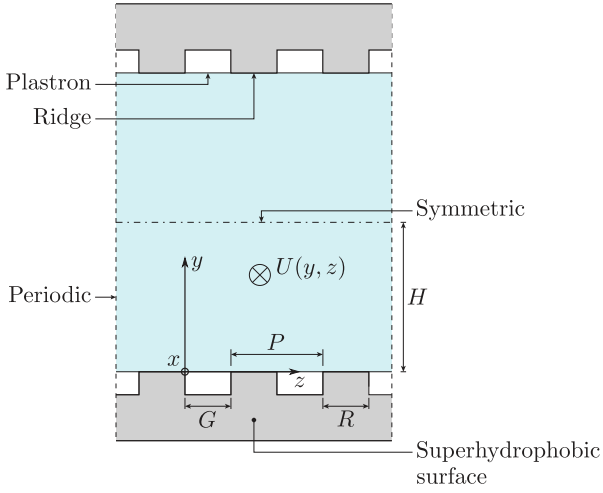


Figure 2. Schematic of the channel flow configuration. An incompressible liquid flows through a plane channel assumed infinitely wide in the transverse z direction. Top and bottom walls are made of long, parallel, periodic superhydrophobic ridges, such that the liquid is in the (suspended) Cassie-Baxter state. A shear-free condition is assumed at the plastrons and a no-slip condition is assumed at the ridges. The time-averaged fully-developed flow velocity in the longitudinal x direction U is assumed invariant with x , and periodic in the z direction with period P .

the viscous length and $U_\tau = (\tau/\rho)^{1/2}$ is the friction velocity), is much larger than the SHS texture period P . Thus, the SHS texture affects the turbulent bulk flow via averaged quantities only, such as the average longitudinal and spanwise slip lengths (λ_x and λ_z). Our turbulent flow model over the SHS is based on a semi-empirical modification to the log law, where the mean velocity profile, $U^+(y^+)$ in wall units (+), is shifted up by an average slip velocity at the interface and down due to turbulent momentum transfer (in accordance with Fukagata *et al.* (2006))

$$U^+(y^+) = \frac{1}{\kappa} \ln(y^+) + B + \Delta U^+, \quad (3)$$

where $\kappa \approx 0.41$ is the von Kármán parameter, $B \approx 5.3$ is an empirical constant, and ΔU^+ is the combined shift relative to the no-slip flow. For the no-slip flow we instead have the classical log law (Pope (2000))

$$U_0^+(y_0^+) = \frac{1}{\kappa} \ln(y_0^+) + B, \quad (4)$$

where the subscript 0 implies that these variables have instead been normalised with wall units that are associated with the flow over a solid wall. For the boundary layer flows considered herein, the log laws (3)–(4) could be extended to include a wake function (Pope (2000)). However, if we assume that the wake function is the same over both a SHS and solid wall, then these terms will cancel in the drag reduction calculation.

The combined shift ΔU^+ has been shown to be well represented by the streamwise slip length (which is equal to the slip velocity in wall units) and by a function of the spanwise slip length, which we denote λ_x^+ and $g(\lambda_z^+)$, such that $\Delta U^+ = \lambda_x^+ + g(\lambda_z^+)$ (Fukagata *et al.* (2006); Busse & Sandham (2012)). When the viscous sublayer is thick compared to

the period of the SHS (see Figures 1 and 2), then

$$\lambda_x^+ = \frac{P^+}{\pi} \ln \left(\sec \left(\frac{\pi\phi}{2} \right) \right), \quad (5)$$

where λ_x^+ is modelled using steady unidirectional laminar flow (Philip (1972); Türk *et al.* (2014)), since the flow in the viscous sublayer is dominated by viscosity. Various approaches have been employed to prescribe $g(\lambda_z^+)$. The saturation as $\lambda_z^+ \rightarrow \infty$ is captured using a formula inspired by riblet technologies (Luchini *et al.* (1991); Busse & Sandham (2012))

$$g(\lambda_z^+) = \frac{-4\lambda_z^+}{4 + \lambda_z^+}. \quad (6)$$

An alternative relationship for $g(\lambda_z^+)$ was proposed by Fukagata *et al.* (2006), whereby g depended exponentially on λ_z^+ . We choose to employ the relationship of Busse & Sandham (2012) because of its simplicity and of its connections with the literature on drag reduction using riblets (Luchini *et al.* (1991)).

We close the above model by assuming that both λ_x^+ and λ_z^+ are based on the laminar solution (5) due to Philip (1972), for longitudinal and transverse shear flows over parallel grooves, such that $\lambda_z^+ = \lambda_x^+/2$ with λ_x^+ in (5). A similar closure hypothesis was made for flows over riblets (Luchini *et al.* (1991); Ibrahim *et al.* (2021)). The normalisation of the average longitudinal slip length in wall coordinates is well defined through $\lambda_x^+ = \lambda_x/\delta_\tau$. However, the normalisation of the average spanwise slip length in wall coordinates, λ_z^+ , is more subtle (Türk *et al.* (2014); Seo & Mani (2016)). We assume that the spanwise velocity fluctuations at the origin of the spanwise turbulent momentum transfer scale with the longitudinal velocity fluctuations. This assumption is commonly made for wall turbulent boundary layers (Pope (2000)). This assumption implies that the outer flow is homogenised in such a way that the average and fluctuating bulk shear stresses in the longitudinal and spanwise directions are of the same order of magnitude. Therefore, we can normalise both the longitudinal and spanwise average slip lengths using the viscous length δ_τ .

To summarise, we can determine the bulk Reynolds number of the SHS flow Re from the shifted log law (3), employing the analytical solutions due to Philip (1972) that describe the streamwise and spanwise slip length in terms of the SHSs geometry, ϕ , P and H (or δ_b). Next, we can evaluate the bulk Reynolds number of the no-slip flow Re_0 from the standard log law (4). The expressions for the SHS and no-slip Reynolds numbers are substituted into the constant-flow-rate assumption, $Re = Re_0$, which when combined with (2) allows one to evaluate the drag reduction.

To incorporate surfactant effects in turbulent flows over SHSs, we modify the slip lengths to account for Marangoni stresses generated by surfactant adsorbed on the air-water interfaces. We leverage recent progress on the modelling of surfactant-induced Marangoni stresses on SHSs for two-dimensional and three-dimensional periodic geometries (Landel *et al.* (2020); Temprano-Coleto *et al.* (2021)). By linearising for small concentrations of surfactant, we can relate the average streamwise slip length λ_x to the average Marangoni shear rate along the interface γ_{Ma} , by solving two-dimensional boundary value problems using conformal mappings (Philip (1972)). The surfactant thereby affects the log law through a change in ΔU^+ . As γ_{Ma} increases, the surface becomes immobile and as $\gamma_{Ma} \rightarrow 0$ we recover the nominal slip length for

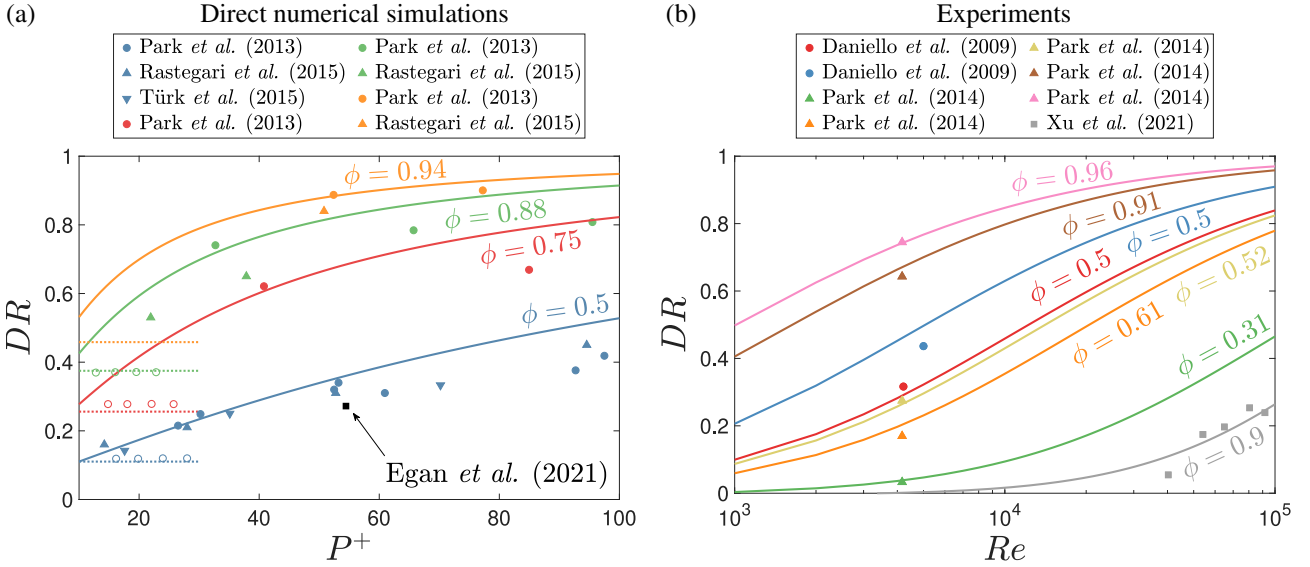


Figure 3. Comparison of our model with (a) numerical and (b) experimental results in the literature, for different gas fractions, ϕ , where the average Marangoni shear rate $\gamma_{Ma} = 0$ and surfactant based effects are neglected. DR is the drag reduction, P^+ is the pitch in wall units and Re is the Reynolds number. Open symbols and dashed lines represent laminar simulations and theory in panel (a), whereas, filled symbols and solid lines represent turbulent simulations and theory in panels (a) and (b).

a clean (surfactant-free) interface. The dependence of γ_{Ma} on the geometry and properties of fluid and surfactant can be attained using the scaling theory detailed in Landel *et al.* (2020) and Temprano-Coletto *et al.* (2021). We study the effect of surfactant by changing the average Marangoni shear rate γ_{Ma} , thus modifying the average streamwise slip length λ_x^+ .

RESULTS AND DISCUSSION

In Figure 3(a) we observe a comparison between the drag reduction predicted by our model (excluding surfactant, such that the average Marangoni shear rate $\gamma_{Ma} = 0$) and direct numerical simulations (exclusive of surfactant), as a function of the SHS period in wall units $P^+ \in [0, 200]$ and gas fraction $\phi = 0.5, 0.75, 0.88$ and 0.94 . We note a regime transition from those laminar simulations which do not vary with P^+ (open symbols and dashed lines), to those with a thick viscous sublayer (filled symbols and solid lines), where the drag reduction increases rapidly with P^+ . The transition from laminar to thick viscous sublayer turbulent flow is associated with the formulation of a turbulent boundary layer, characterised by the viscous length scale δ_τ . Due to the limited amount of numerical data for $\phi > 0.5$, it is not possible to comment on the dependence of the transition on the gas fraction. In Figure 3(a), the drag reduction increases with increasing gas fraction. The agreement is good for $0 \lesssim P^+ \lesssim 50$, however, for $P^+ \gtrsim 50$, another regime transition seems to occur, with the drag reduction tending to saturate, in contrast with the model which increases to 100% drag reduction for $P^+ \rightarrow \infty$. This is not unexpected, as our model assumes that the viscous sublayer thickness, of order $10\delta_\tau$, is much larger than the SHS texture period P .

As previously noted, a limitation of the above model is that $DR \rightarrow 1$ as the Reynolds number $Re \rightarrow \infty$. Recent simulations, however, suggest that the drag reduction saturates for increasing P^+ (Park *et al.* (2013); Türk *et al.* (2014); Rastegari & Akhavan (2015)) - see Figure 3(a). It seems reasonable to assume that in the limit as $Re \rightarrow \infty$, there exists an upper bound given by $DR \rightarrow \phi$, as also discussed by Daniello *et al.* (2009); Rothstein (2010). As the Reynolds number increases,

the thickness of the viscous sublayer is reduced and the SHSs will have a greater effect on the streamwise velocity (that acts to reduce the drag) whilst reducing spanwise momentum transfer (that acts to increase the drag). Returning to our model, we propose taking the drag reduction to be the minimum value $\min(DR, \phi)$, which improves model predictions significantly for large P^+ .

We also performed numerical simulations for turbulent channel flows over SHSs on a dynamically adapted forest of Octree grids in a parallel environment based on Egan *et al.* (2021) - see the black data point in Figure 3(a). An extension of this algorithm, which couples the velocity and pressure to bulk and interfacial surfactant evolution, is currently under development to give further insight into the role of surfactants in turbulent flows over SHSs.

We compare the drag reduction predicted by our model with experimental data in Figure 3(b) for $Re \in [10^3, 10^5]$ and $\phi \in [0.31, 0.96]$. The experimental works of Park *et al.* (2014) and Xu *et al.* (2021) consider external flows, for which a turbulent boundary layer thickness must first be obtained in order to evaluate DR . We assume that the turbulent boundary layer thickness may be approximated by the classical result from turbulent boundary-layer theory (Schlichting & Gersten (2003))

$$\delta_b = \frac{0.37x}{Re_x^{1/5}} \quad (7)$$

where $Re_x = Ux/\nu$ is the Reynolds number (U is the bulk velocity and ν is the kinematic viscosity). Equation (7) is evaluated at a fixed central location down the test section, x , in order to calculate the drag reduction. This highlights an important difference in external flows, where the ratio δ_b/P varies greatly comparing the brown curves of Park *et al.* (2014) and the grey curves of Xu *et al.* (2021). The large change in δ_b/P is due to the test section being much longer in Xu *et al.* (2021), which causes the drag reduction to be much smaller even though $\phi = 0.9$ does not change. Our model captures the variation of drag reduction with respect to the gas fraction in

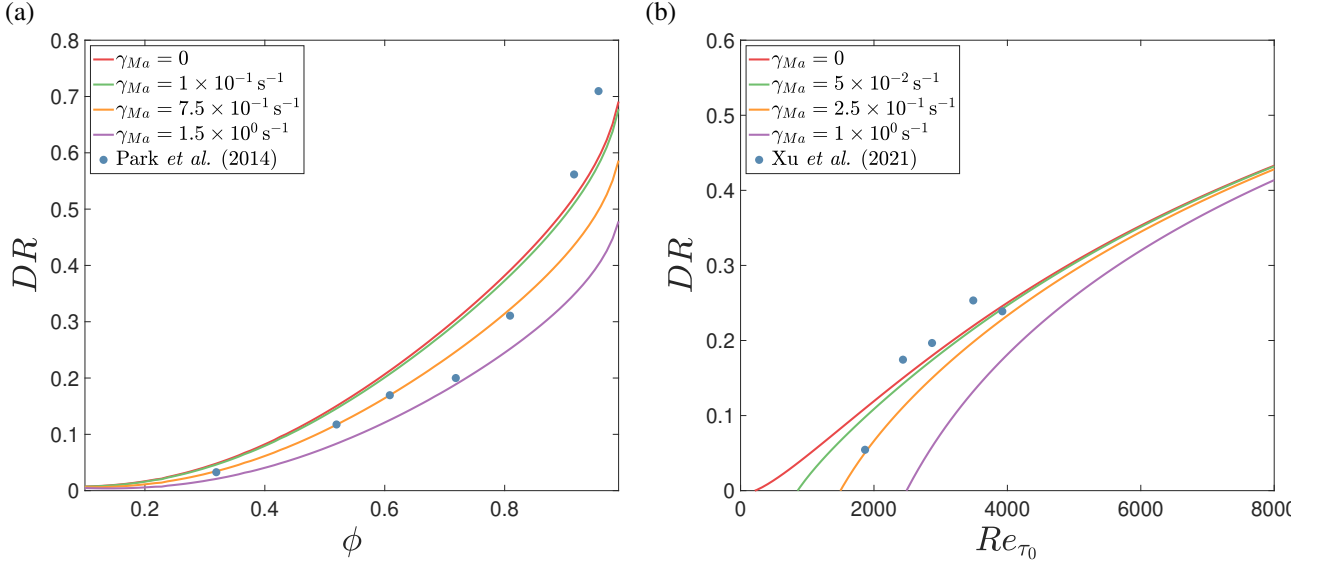


Figure 4. Comparison of our model with the experimental results in turbulent boundary layers (a) Park *et al.* (2014) and (b) Xu *et al.* (2021), for different average Marangoni shear rates, γ_{Ma} . DR is the drag reduction, ϕ is the gas fraction and Re_{τ_0} is the friction Reynolds number (normalised with wall units associated with the flow over a solid wall). Filled symbols and solid lines represent turbulent experimental data and theory respectively in panels (a) and (b).

the experiments of Park *et al.* (2014) (see the green, orange, yellow, brown and pink curves in Figure 3(b)). There is significant spread in the original experimental data of Daniello *et al.* (2009) which could be due to a number of features of SHSs, e.g. liquid-gas interface curvature, the gas subphase, loss of plastron, ridge alignment (Park *et al.* (2021)). In Figure 3(b), we show an ensemble average of the DR data extracted from Daniello *et al.* (2009) over Re , in a similar manner to Park *et al.* (2021), in order to ease the comparison between this data and the other experiments.

We investigate the effect of average Marangoni shear rate γ_{Ma} on the model predictions, where we find that the introduction of surfactant impairs the drag reduction DR , but does not generally improve the model predictions when compared to a clean channel - see Figures 4 and Table 1. One would expect the effect of surfactant to be more prominent in fieldwork than in a laboratory setting, where the water is relatively clean. Surfactant effects are quantified via the root mean squared error ϵ_{RMS} comparing the drag reduction predicted by our model

Park <i>et al.</i> (2014)		Xu <i>et al.</i> (2021)	
γ_{Ma} (s^{-1})	ϵ_{RMS}	γ_{Ma} (s^{-1})	ϵ_{RMS}
0	0.0052	0	0.0010
1×10^{-1}	0.0052	5×10^{-2}	0.0009
7.5×10^{-1}	0.0090	2.5×10^{-1}	0.0019
1.5×10^0	0.0210	1×10^0	0.0215

Table 1. The root mean square error of our model, ϵ_{RMS} , comparing the drag reduction predicted by our model DR_{Model} to the drag reduction predicted by experimental data DR_{Data} , considering experimental results in turbulent boundary layers (a) Park *et al.* (2014) or (b) Xu *et al.* (2021), for different average Marangoni shear rates, γ_{Ma} .

DR_{Model} to the drag reduction predicted by experimental data DR_{Data} in Table 1. We see that for the data in Park *et al.* (2014) and Xu *et al.* (2021), the predictions for small γ_{Ma} give a smaller root mean squared error than those for a clean channel $\gamma_{Ma} = 0$. However, any decrease in ϵ_{RMS} is not statistically significant and lies within the experimental uncertainty of the results. The limited data and lack of experiments including surfactant makes the experimental results difficult to interpret. More accurate experiments are therefore required to infer whether surfactants will be important in turbulent applications, as several additional features could be involved and causing the changes in drag; e.g. liquid-gas interface curvature, the gas subphase, loss of plastron, or ridge alignment (Park *et al.* (2021)). Our findings also call for turbulent direct numerical simulations inclusive of surfactants, which, as previously mentioned, we are currently pursuing.

CONCLUSIONS

Motivated by recent developments that demonstrate the importance of surfactants in laminar flows over SHSs (Kim & Hidrovo (2012); Bolognesi *et al.* (2014); Peaudecerf *et al.* (2017); Song *et al.* (2018); Landel *et al.* (2020)), we have proposed a model for turbulent flow that includes surfactant based on a shifted log law (Fukagata *et al.* (2006)). We consider both channel and boundary layer flows over SHSs, in order to compare with the wide range of numerical and experimental results in the literature. The model assumes that the viscous sublayer thickness is much larger than the SHS texture period P and, therefore, that the SHS texture affects the turbulent bulk flow via averaged quantities only, such as the average longitudinal and spanwise slip lengths. Our model employs an empirical relationship for the saturation of the transverse slip length based on riblet theory (Luchini *et al.* (1991); Busse & Sandham (2012)). Using the analytical solutions due to Philip (1972), we can then use our model to relate the drag reduction directly to the geometry of the SHS and properties of the surfactant.

We compare our model predictions with direct numerical simulations, where there is an agreement in the drag reduction for small P^+ (in wall units $+$). The model captures the dependence of the drag reduction on the geometry of the SHS and channel height (or boundary layer thickness). This holds until we transition into a different regime where the drag reduction from the direct numerical simulations asymptotically approaches the gas fraction for $P^+ \rightarrow \infty$. We also compare our model predictions with experimental data, which allows us to investigate surfactant effects in turbulent flows over SHSs. In addition, the model demonstrates that the presence of surfactant is detrimental to the drag reduction at all gas fractions, where greater reductions in drag are seen at smaller Reynolds numbers. From the comparison between a surfactant-inclusive model and the experimental data found in the literature, we do not have sufficient evidence to conclude that surfactants have affected the drag reduction performance of the SHS studied. The differences between experimental findings are better explained by changes in the ratio between the boundary layer thickness and the SHS texture period. For shorter gratings (which are necessary at high speeds) and higher surfactant concentrations (which are common in maritime environments), our model suggests that surfactant may become important again. More numerical and experimental work should be conducted to further disentangle the effect of surfactant in turbulent flows over SHSs.

ACKNOWLEDGEMENTS

We gratefully acknowledge support from CBET-EPSRC (NSF #2054894, EPSRC Ref. EP/T030739/1), and partial support from ARO MURI W911NF-17-1-0306.

REFERENCES

- Bolognesi, G, Cottin-Bizonne, C & Pirat, C 2014 Evidence of slippage breakdown for a superhydrophobic microchannel. *Phys. Fluids* **26** (8), 082004.
- Busse, A & Sandham, N D 2012 Influence of an anisotropic slip-length boundary condition on turbulent channel flow. *Phys. Fluids* **24**, 055111.
- Crowdy, D. G. 2017 Perturbation analysis of subphase gas and meniscus curvature effects for longitudinal flows over superhydrophobic surfaces. *J. Fluid Mech.* **822**, 307.
- Daniello, R.J., Waterhouse, N.E. & Rothstein, J.P. 2009 Drag reduction in turbulent flows over superhydrophobic surfaces. *Phys. Fluids* **21** (8), 085103.
- Egan, R, Guittet, A, Temprano-Coleto, F, Isaac, T, Peaudecerf, F J, Landel, J R, Luzzatto-Fegiz, P, Burstedde, C & Gibou, F 2021 Direct numerical simulation of incompressible flows on parallel octree grids. *J. Comp. Phys.* **428**, 110084.
- Fukagata, K, Kasagi, N & Koumoutsakos, P 2006 A theoretical prediction of friction drag reduction in turbulent flow by superhydrophobic surfaces. *Phys. Fluids* **18** (5), 051703.
- Fukuda, K., Tokunaga, J., Nobunaga, T., Nakatani, T., Iwasaki, T. & Kunitake, Y. 2000 Frictional drag reduction with air lubricant over a super-water-repellent surface. *J. Mar. Sci. Technol.* **5**, 123–130.
- Gose, J.W., Golovin, K., Boban, M., Mabry, J.M., Tuteja, A., Perlin, M. & Ceccio, S.L. 2018 Characterization of superhydrophobic surfaces for drag reduction in turbulent flow. *J. Fluid Mech.* **845**, 560.
- Ibrahim, J. I., Gomez-de Segura, G., Chung, D. & Garcia-Mayoral, R. 2021 The smooth-wall-like behaviour of turbulence over drag-altering surfaces: a unifying virtual-origin framework. *J. Fluid Mech.* **915**.
- Kim, T J & Hidrovo, C 2012 Pressure and partial wetting effects on superhydrophobic friction reduction in microchannel flow. *Phys. Fluids* **24** (11), 112003.
- Landel, J.R., Peaudecerf, F.J., Temprano-Coleto, F, Gibou, F, Goldstein, R.E. & Luzzatto-Fegiz, P 2020 A theory for the slip and drag of superhydrophobic surfaces with surfactant. *J. Fluid Mech.* **883**, A18.
- Luchini, P., Manzo, F. & Pozzi, A. 1991 Resistance of a grooved surface to parallel flow and cross-flow. *J. Fluid Mech.* **228**, 87–109.
- Park, H., Choi, C.-H. & Kim, C.-J. 2021 Superhydrophobic drag reduction in turbulent flows: a critical review. *Exp. Fluids* **62**, 229.
- Park, H, Park, H & Kim, J 2013 A numerical study of the effects of superhydrophobic surface on skin-friction drag in turbulent channel flow. *Phys. Fluids* **25** (11), 110815.
- Park, H, Sun, G & Kim, C-J 2014 Superhydrophobic turbulent drag reduction as a function of surface grating parameters. *J. Fluid Mech.* **747**, 722.
- Peaudecerf, F J, Landel, J R, Goldstein, R E & Luzzatto-Fegiz, P 2017 Traces of surfactants can severely limit the drag reduction of superhydrophobic surfaces. *P. Nat. Acad. Sci. USA* **114**, 7254.
- Philip, J.R. 1972 Flows satisfying mixed no-slip and no-shear conditions. *Z. Angew. Math. Physik* **23** (?), 353.
- Pope, S B 2000 *Turbulent Flows*. Cambridge University Press.
- Rastegari, A & Akhavan, R 2015 On the mechanism of turbulent drag reduction with super-hydrophobic surfaces. *J. Fluid Mech.* **773**.
- Rastegari, A & Akhavan, R 2019 On drag reduction scaling and sustainability of superhydrophobic surfaces in high Reynolds number turbulent flows. *J. Fluid Mech.* **864**, 327.
- Rothstein, J.P. 2010 Slip on superhydrophobic surfaces. *Ann. Rev. Fluid. Mech.* **42**, 89.
- Schlichting, H. & Gersten, K. 2003 *Boundary-layer theory*. Springer Science & Business Media.
- Seo, J. & Mani, A. 2016 On the scaling of the slip velocity in turbulent flows over superhydrophobic surfaces. *Phys. Fluids* **28** (2), 025110.
- Smith, TWP, Jalkanen, JP, Anderson, BA, Corbett, JJ, Faber, J, Hanayama, S, O'keeffe, E, Parker, S, Johansson, L, Aldous, L *et al.* 2015 Third imo greenhouse gas study 2014 .
- Song, D, Song, B, Hu, H, Du, X, Du, P, Choi, C-H & Rothstein, J P 2018 Effect of a surface tension gradient on the slip flow along a superhydrophobic air-water interface. *Phys Rev Fluids* **3** (3), 033303.
- Temprano-Coleto, F, Smith, S M, Peaudecerf, F J, Landel, J R, Gibou, F & Luzzatto-Fegiz, P 2021 Slip on three-dimensional surfactant-contaminated superhydrophobic gratings. *arXiv preprint arXiv:2103.16945* .
- Teo, C J & Khoo, B C 2009 Analysis of Stokes flow in microchannels with superhydrophobic surfaces containing a periodic array of micro-grooves. *Microfluid* **7**, 353.
- Türk, S., Daschiel, G., Stroth, A., Hasegawa, Y. & Frohnapfel, B. 2014 Turbulent flow over superhydrophobic surfaces with streamwise grooves. *J. Fluid Mech.* **747**, 186–217.
- Xu, M., Grabowski, A., Yu, N., Kerezyte, G., Lee, J., Pfeifer, B. R. & Kim, C. 2020 Superhydrophobic drag reduction for turbulent flows in openwater. *Phys. Rev. Appl.* **13** (3).
- Xu, M., Yu, N., Kim, J. & Kim, C. 2021 Superhydrophobic drag reduction in high-speed towing tank. *J. Fluid Mech.* **908**.